

Alma Mater Studiorum Università di Bologna
Archivio istituzionale della ricerca

Improving the flexibility and compostability of starch/poly(butylene cyclohexanedicarboxylate)-based blends

This is the final peer-reviewed author's accepted manuscript (postprint) of the following publication:

Published Version:

Franco Dominici, M.G. (2020). Improving the flexibility and compostability of starch/poly(butylene cyclohexanedicarboxylate)-based blends. CARBOHYDRATE POLYMERS, 246, 1-8 [10.1016/j.carbpol.2020.116631].

Availability:

This version is available at: <https://hdl.handle.net/11585/790943> since: 2021-01-24

Published:

DOI: <http://doi.org/10.1016/j.carbpol.2020.116631>

Terms of use:

Some rights reserved. The terms and conditions for the reuse of this version of the manuscript are specified in the publishing policy. For all terms of use and more information see the publisher's website.

This item was downloaded from IRIS Università di Bologna (<https://cris.unibo.it/>).
When citing, please refer to the published version.

(Article begins on next page)

1 **Improving the flexibility and compostability of**
2 **starch/poly(butylene cyclohexanedicarboxylate)-based blends**

3
4 Franco Dominici^{a,1}, Matteo Gigli^{b,1,*}, Ilaria Armentano^c, Laura Genovese^d, Francesca Luzi^a, Luigi
5 Torre^a, Andrea Munari^d, Nadia Lotti^{d,*}
6
7
8
9
10

11 ^aCivil and Environmental Engineering Department, University of Perugia, UdR INSTM, Terni (Italy)

12 ^bDepartment of Molecular Sciences and Nanosystems, Ca'Foscari University of Venice, Venice
13 (Italy)

14 ^cDepartment of Economics, Engineering, Society and Business Organization (DEIm), University of
15 Tuscia, Viterbo (Italy)

16 ^dCivil, Chemical, Environmental and Materials Engineering Department, University of Bologna,
17 Bologna (Italy)
18
19
20
21
22
23

24 ¹*Equally contributing authors*

25 *Correspondence to: Tel: +39 041 2348655; +39 051 2090354

26 e-mail address: matteo.gigli@unive.it; nadia.lotti@unibo.it
27
28
29
30
31
32
33

34 **Abstract**

35 Fully biobased blends of thermoplastic starch and a poly(butylene cyclohexanedicarboxylate)-based
36 random copolyester containing 25% of adipic acid co-units (PBCEA) are prepared by melt blending
37 and direct extrusion film casting. The obtained films are characterized from the physicochemical and
38 mechanical point of view and their fragmentation under composting conditions is evaluated. The
39 results demonstrate that the introduction of adipic acid co-units in the PBCE macromolecular chains
40 permits to decrease the blending temperature, thus avoiding unwanted starch degradation reactions.
41 Moreover, the presence of small amounts of citric acid as compatibilizer further improves the
42 interfacial adhesion between the two components and promotes the formation of micro-porosities
43 within the films. The synergistic combination of these factors leads to the development of materials
44 showing an elastomeric behavior, i.e. no evident yield and elongation at break higher than 450%,
45 good moisture resistance and fast fragmentation in compost.

46

47

48

49

50

51

52

53

54

55 **Keywords**

56 Thermoplastic starch (TPS), poly(butylene cyclohexanedicarboxylate), compatibilization, biobased
57 polymer blends, elastomeric behavior

58

59

60

61

62

63

64

65

66

67

68 1. Introduction

69 The growing environmental concern about (micro)plastic pollution even in remote regions of our
70 planet is posing great attention on the urgent need of reducing the employment of long-lasting
71 polymeric materials. Especially for the fabrication of disposable items, where indefinite in-service
72 durability is not required, biodegradable plastics may represent a solution.(Kabir et al., 2020) The
73 combination of biodegradability and biobased character is even more desirable, as it would permit to
74 limit the dependence on fossil resources and facilitate the transition towards a circular economy. In
75 the last decades, many biopolymers have attracted considerable interest and have been studied for the
76 production of sustainable formulations with comparable (or superior) technical performances and
77 competitive costs with respect to traditional materials.(RameshKumar et al., 2020; Yin & Yang, 2020)
78 Among various possibilities, starch has been widely used due to its low cost and high
79 abundance.(Ojogbo et al., 2020) It is in fact produced by many plants and stored in the cells as source
80 of energy.(H. Liu et al., 2009) However, due to strong intermolecular interactions, starch in its native
81 form is not thermoplastic. Therefore, it must be processed, through the joint action of plasticizers
82 such as glycerol and water, heat and shear stress, into a workable plastic material.(Khan et al., 2017)
83 If, in principle, 100% thermoplastic starch (TPS) films can be produced, some important drawbacks,
84 i.e. moisture sensitivity, which causes starch recrystallization, and poor mechanical properties,
85 hamper their applicability.(Ojogbo et al., 2020) In the attempt of better exploiting the favorable
86 characteristics of starch, TPS has been blended, most commonly via melt blending, with a wide range
87 of polymers. Studies include oil-derived commodities and greener alternatives, being aliphatic and
88 aliphatic/aromatic polyesters the most explored options.(Kaseem et al., 2012) In particular, much
89 research has focused on commercially available (co)polyesters like polylactic acid,(Zaaba & Ismail,
90 2019) polyhydroxyalcanoates,(Parulekar & Mohanty, 2007) polycaprolactone,(Bulatović et al., 2019;
91 Ortega-Toro et al., 2016) poly(butylene succinate),(Lai et al., 2005) and poly(butylene adipate-*co*-
92 terephthalate).(Ivanič et al., 2019; Wang et al., 2015; Wei et al., 2015)

93 **Aiming at obtaining TPS-rich blends with high flexibility and low retrogradation issues, in this**
94 **contribution another approach, that deviates from the commonly adopted strategies, has been chosen.**
95 **Instead of employing existing polymeric matrices and then working on the compatibilization between**
96 **the blend components by further chemical modification of the polymer or by adding significant**
97 **amounts of other compounds that act as compatibilizers, a tailor-made polyester, i.e. a poly(butylene**
98 **cyclohexanedicarboxylate-*co*-adipate) copolymer (PBCEA), has been synthesized to achieve the**
99 **desired properties.**

100 The two acid subunits, their molar ratio and the polymer architecture have been specifically selected
101 for the following reasons. On the one hand, poly(butylene cyclohexanedicarboxylate) (PBCE) is

102 characterized by the presence of a cycloaliphatic ring in the repeating unit, whose structure resembles
103 the glucose molecule and may thus improve the compatibility with starch. This polyester displays
104 high melting temperature and good resistance to heat, light and moisture, making it very appealing
105 for uses as packaging material.(Gigli et al., 2013; Gigli, Lotti, et al., 2014) **Additionally**, both
106 monomers leading to PBCE can be obtained from renewable resources, i.e. from succinic acid and
107 limonene-derived terephthalic acid.(Genovese et al., 2016) On the other hand, adipic acid, it too
108 potentially biobased,(Skoog et al., 2018) has been randomly introduced along the PBCE main chain
109 with the aim of lowering the melting of the crystalline domains. This way the blending temperature
110 can be decreased, thus avoiding any undesired starch degradation through the combined action of
111 heat and shear stress, with a consequent decline of its properties.(W.-C. Liu et al., 2010)
112 To further increase the miscibility between the blend components, **low amounts** of citric acid (CA)
113 have been added to the formulation, as CA promotes the fragmentation and dissolution of starch
114 granules by crosslinking, (trans)esterification and hydrolysis reactions during melt
115 compounding.(Carvalho et al., 2005; Ghanbarzadeh et al., 2011; Shi et al., 2007)
116 Films with a fixed 50:50 composition between PBCEA and TPS and different amount of CA have
117 been prepared by melt blending and direct film casting, and subsequently characterized from the
118 molecular, morphological, thermal and mechanical point of view. Surface wettability and moisture
119 absorption have been also investigated. Lastly, end-of-life fate of the developed materials has been
120 evaluated by lab-scale composting studies over 4-weeks period.

121

122 **2. Materials and methods**

123 *2.1 Materials*

124 *Trans*-cyclohexane-1,4-dicarboxylic acid (CHDA, 98%) and adipic acid (AA, 99%) were purchased
125 from TCI Chemicals (Tokyo, Japan), glycerol (99%) from Alfa Aesar (Haverhill, MA, USA), while
126 wheat starch (WS), 1,4-butanediol (BD, 99%), citric acid (CA, 99.5%) and titanium tetrabutoxide
127 (TBT, 97%) from Sigma-Aldrich (Milan, Italy). TBT was distilled before use, while all the other
128 compounds were used as received.

129 *2.2 Polymer synthesis and starch plasticization*

130 PBCEA was synthesized through two-step melt polycondensation. CHDA, AA and BD in molar ratio
131 0.75:0.25:1.4 were added to a 200 mL glass reactor together with the catalyst (TBT, 100 ppm/g of
132 polymer) and 0.1% wt. of glycerol (with respect to theoretical polymer mass). The reaction mixture,
133 kept under nitrogen atmosphere, was heated to 180°C in a **thermostated** salt-based bath and allowed
134 to proceed until more than 90% of the theoretical water distilled off. In the second step, the pressure

135 was gradually reduced to 0.1 mbar and the temperature increased to 240°C. The polymerization was
136 stopped when the torque, continuously recorded during the reaction, reached a constant value.

137 Wheat starch plasticization was performed as previously described.(Genovese et al., 2018) Briefly,
138 72% wt. of wheat starch was mixed in a co-rotating twin screw extruder (DSM Explorer 5&15 CC
139 Micro Compounder) with 28% wt. of glycerol for 3 min at 30 rpm, with a temperature profile of 135-
140 140-145°C. The obtained TPS filament was pelletized to be used for blend preparation.

141 *2.3 Blend processing and filming procedure*

142 PBCEA and TPS were separately pelletized and dried under vacuum at 50 °C for 24 h. Three blend
143 formulations, in addition to pristine PBCEA, were developed (**Table 1**). A polymer ratio equal to
144 50% wt. of PBCEA was selected based on previous results and different concentrations of CA (0.5
145 and 1.0% wt.) as compatibilizer have been tested.(Genovese et al., 2018)

146 The microextruder was used in speed control mode at 50 rpm to achieve the melt blending of PBCEA
147 and TPS. PBCEA was first introduced in the compounder, while TPS was added after 2 mins. Mixing
148 was then continued for 1 additional minute. The temperature profile in the three zones of the extruder
149 was set to 150-155-165°C to obtain adequate conditions for subsequent direct filming. For this last
150 step, the compounder was switched in force control mode, and a microfilm die coupled with a casting
151 film line (DSM Film Device) was added. The processing parameters to produce cast films were
152 modified according to the rheological behavior of the blends, as reported in **Table 1**, under constant
153 speed (500 mm min⁻¹) and torque (40 Nmm). Films of about 100-120 µm thickness were obtained.

154

155 **Table 1.** Formulations and film processing parameters of PBCEA/TPS blends

Sample	PBCEA (% wt.)	TPS (% wt.)	CA (% wt.)	Force (N)
PBCEA	100	0	0	650
PBCEA/TPS	50	50	0	750
PBCEA/TPS-CA0.5	50	49.5	0.5	800
PBCEA/TPS-CA1	50	49	1	850

156

157 *2.4 Physicochemical characterization*

158 PBCEA composition was verified by ¹H-NMR on a Varian INOVA 400 MHz instrument (Agilent
159 Technologies). Chloroform-d containing 0.03% (v/v) tetramethylsilane as internal standard was used
160 as solvent with a polymer concentration of about 0.5 %wt. Spectra were collected at RT. The
161 molecular weight and dispersity index (**DI**) were obtained by gel permeation chromatography (GPC)
162 by employing a 1100 Hewlett Packard system (Agilent Technologies) equipped with a PLgel 5 mm
163 MiniMIX-C column and a refractive index detector. Chloroform was used as eluent with a 0.3 mLmin⁻¹

164 ¹ flow. Polystyrene standards in the molecular weight range 4k-200k were used to build the calibration
165 curve.

166 Surface morphology and cross-section were studied on a field emission scanning electron microscope
167 (FE-SEM, SUPRA™ 35, Carl Zeiss SMT) on gold sputtered samples.

168 For cross-section analysis specimens were freeze-cut in liquid nitrogen along the transverse direction.
169 A Jasco FT-IR 615 spectrometer equipped with a Germanium crystal and operating in attenuated total
170 reflection (ATR) mode was employed for infrared (IR) spectrum measurements in the 400-4000 cm⁻¹
171 range.

172 Thermogravimetry (TGA) was carried out under nitrogen atmosphere (30 mLmin⁻¹) on a Perkin
173 Elmer TGA7 apparatus. A heating scan of 10 °Cmin⁻¹ was used for the analysis.

174 Calorimetric analysis was run on a Perkin Elmer DSC6 instrument. Weighed samples were
175 encapsulated in aluminum pans and heated to 180°C. After holding at this temperature for 3 min to
176 delete any thermal history, specimens were quenched to -60 °C and then heated at 20 °Cmin⁻¹ up to
177 160°C (II scan). To determine the crystallization rate under non-isothermal conditions, samples were
178 cooled from the melt (see above) at 5 °Cmin⁻¹.

179 Static water contact angle (WCA) was measured on blend films at room temperature (RT) by using a
180 KSV CAM101 instrument. Side profiles of deionized water drops were recorded for image analysis
181 after 2 s from deposition. Contact angles are reported as the average value of at least ten different
182 measurements.

183 The moisture content (MC) was evaluated at 25 °C and 53% of relative humidity (RH). Measurements
184 were taken after 1 and 5 weeks of incubation. The test was run in triplicate, according to the following
185 procedure: samples measuring 20 × 20 mm were cut and pre-dried under vacuum at 40 °C for 72 h.
186 The films were then placed in desiccators containing Mg(NO₃)₂ till constant weight was detected.
187 MC was estimated according to Eq. 1:

$$188 \quad MC(\%) = \frac{W_{Final} - W_{Initial}}{W_{Final}} \times 100 \quad (\text{Eq. 1})$$

189 where W_{Final} is the weight of sample after 1 or 5 weeks at 53% RH and 25 °C and W_{Initial} is the weight
190 of pre-dried samples.

191 *2.5 Mechanical characterization*

192 Tensile tests were performed on films by employing an Instron 4465 testing machine, equipped with
193 a rubber grip and a 100 N load cell. A preload of 1 MPa and a crosshead speed of 10 mm min⁻¹ were
194 applied. Results are provided as average ± standard deviation of at least 5 replicates.

195 *2.6. Composting*

196 Composting tests were carried out at (58.0 ± 0.1)°C using mature compost supplied by HerAmbiente
197 S.p.A. (Bologna, Italy) and having the following composition (as declared by HerAmbiente): organic

198 carbon: 22.08% of the dry solid, humic and fulvic carbon: 13.44% of the dry solid, C/N ratio: 12.97,
199 pH: 8.15 and salinity: 2.88 dS m⁻¹. Each sample (about 20 × 20 mm in size) was placed in a 100 mL
200 glass bottle in between two layers of compost (20 g each). 10 mL of deionized water was added.
201 Specimens were recovered at determined time intervals, washed accordingly to the procedure
202 previously described,(Genovese et al., 2014) and dried over P₂O₅ under vacuum to constant weight.
203 Weight loss was calculated as follows:

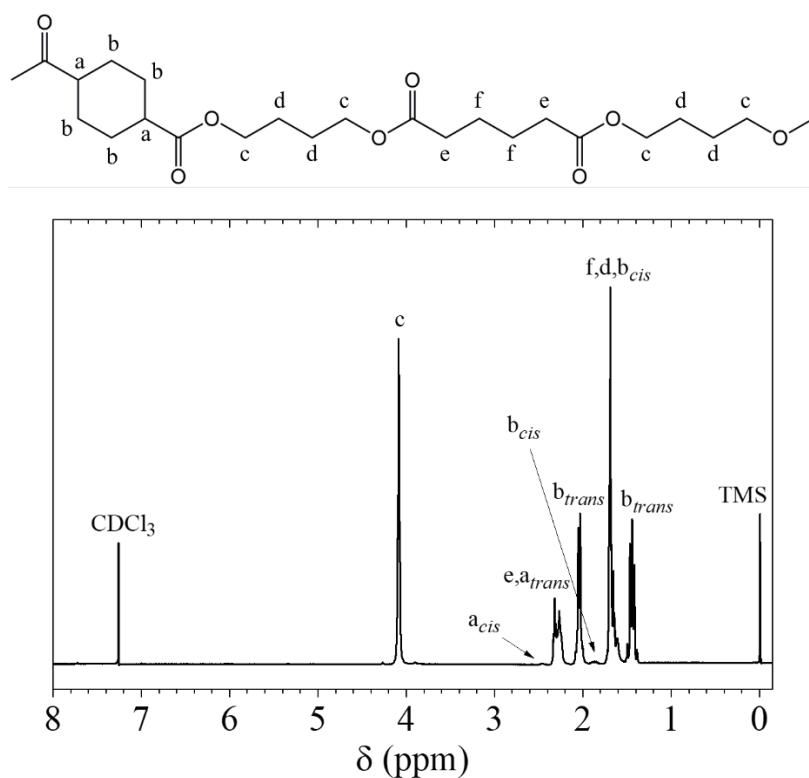
$$((m_i - m_f) / m_i) \times 100 \quad (\text{Eq. 2})$$

204 where m_f and m_i are the final and the initial sample weight, respectively.

206

207 3. Results and Discussion

208 High molecular weight PBCEA ($M_n = 37.5$ kDa, $DI = 2.1$), whose chemical structure was elucidated
209 by ¹H-NMR analysis (Figure 1), was obtained.



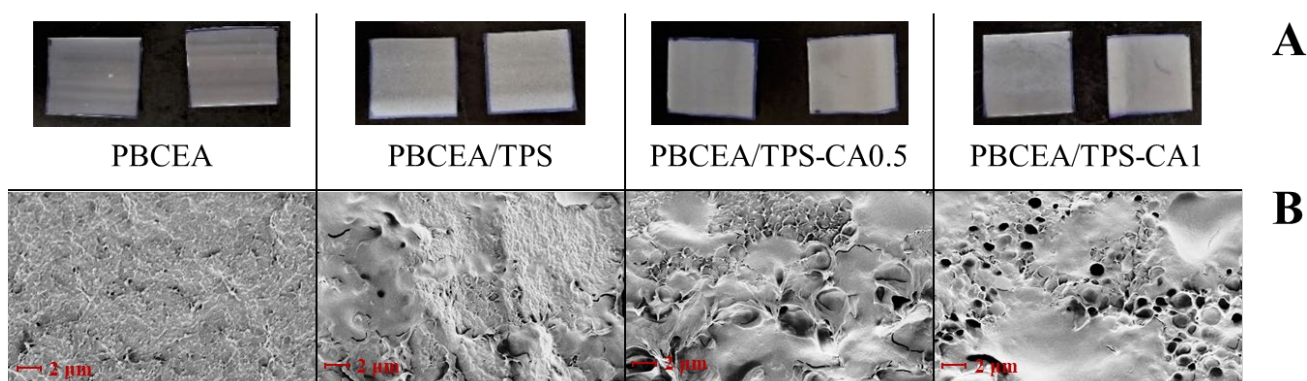
210

211 **Figure 1.** ¹H-NMR spectrum of PBCEA with resonance assignments.

212

213 The copolymer composition, deduced from the integration of the peaks located at 2.27 ppm (e), 2.31
214 ppm (a_{trans}) and 2.46 ppm (a_{cis}) resulted close to the feed (27.8 mol% of butylene adipate co-units).
215 Furthermore, the calculation of the ratio between the area of the b_{cis} (1.87 ppm) and b_{trans} (2.04 ppm)
216 peaks evidenced that no significant isomerization occurred during the reaction as the measured
217 content of *cis* isomer was equal to 2.7%. These results demonstrated that the adopted polymerisation
218 protocol was optimized with respect to previously reported conditions.(F. Liu et al., 2016)

219 All materials were then easily processed into blends and allowed for the production of films suitable
 220 for subsequent characterization. To obtain films of comparable thickness, the counter thrust parameter
 221 (Force, **Table 1**) was optimized for each formulation during the film casting, since the presence of
 222 CA, due to its crosslinking action,(Ghanbarzadeh et al., 2011; Shi et al., 2007) caused an increase in
 223 resistance forces. Defect-free films of variable thickness in the range 30-100 μm (modulated based
 224 on the subsequent characterization technique) have been obtained. Their light colour (**Figure 2A**)
 225 indicates the absence of undesired degradation reactions, e.g. caramelization, during processing.
 226 **Figure 2B** reports the micrographs of the fracture surfaces for PBCEA and PBCEA/TPS blend films.
 227 The cross section of the neat polyester film displays a uniform phase with a few submicrometric
 228 cavities, which can be due to the evaporation of low molecular weight residues from the synthesis
 229 step. As to the PBCEA/TPS blend, a better dispersion between the two phases with respect to other
 230 PBCE-based blends of similar composition previously investigated can be observed.(Genovese et al.,
 231 2018) However, phase separation highlighted by the presence of some cracks and detachments, is still
 232 present. The addition of CA during compounding improves interface adhesion. Indeed, numerous
 233 trabecular connections are identified between the two polymers. On the other hand, the concentration
 234 and size of the cavities rise, probably because of degradation and (trans)esterification reactions
 235 occurring during reactive extrusion in the presence of CA.(Olivato et al., 2014)
 236 A further increase of the CA content makes the above described phenomena more evident. Indeed, a
 237 better binding of the two phases is reached, but an increment of the number of voids, which are mainly
 238 located in the PBCEA phase, can be concomitantly observed. Therefore, the morphological analysis
 239 suggests that CA, during the reactive extrusion, exerts a double function.

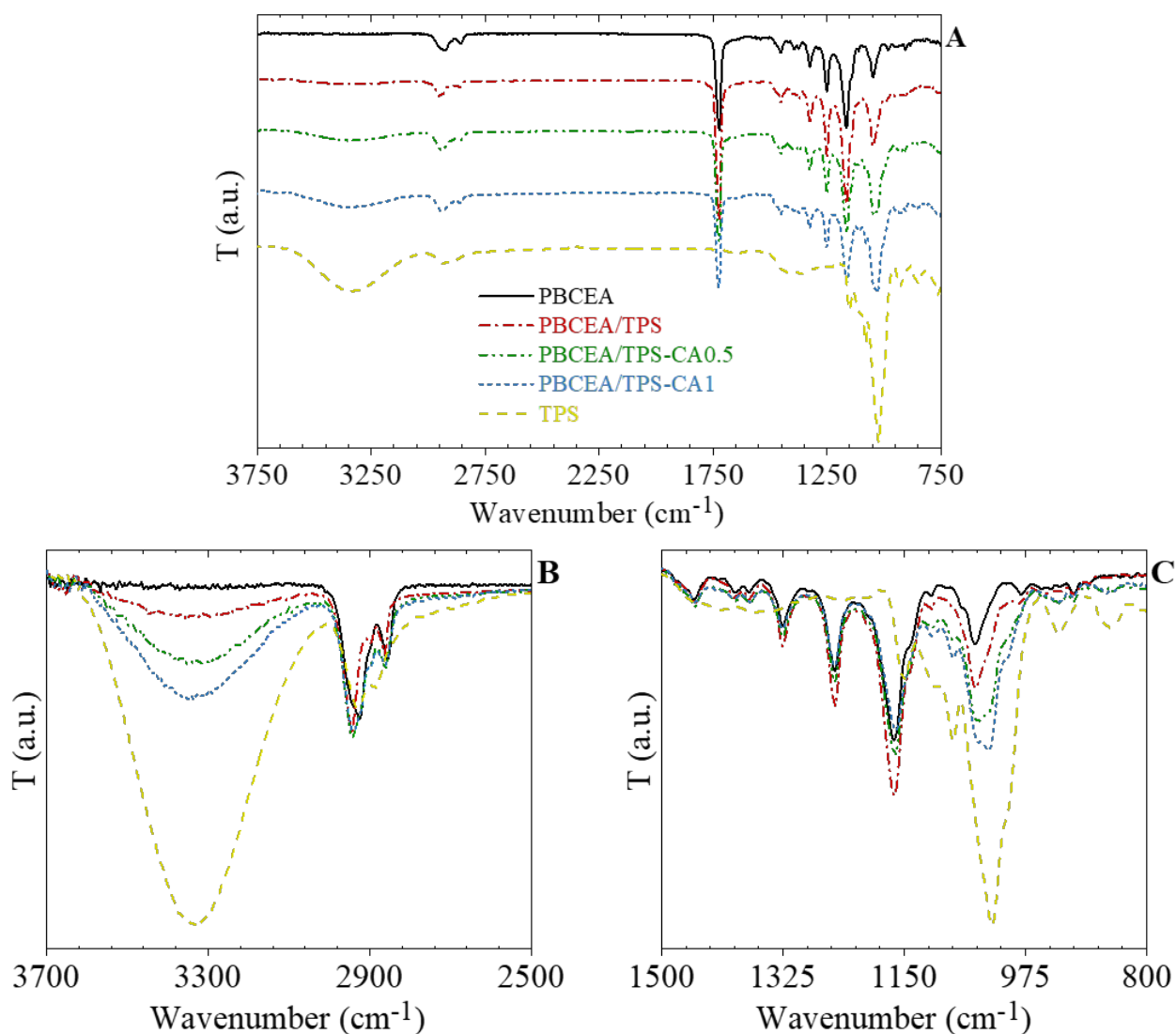


240
 241 **Figure 2.** A) Photographs of PBCEA and PBCEA/TPS films. Squares of about 9 cm^2 are depicted.
 242 B) FESEM micrographs of the cross sections of PBCEA and PBCEA/TPS blends.

243
 244 On the one hand, owing to crosslinking and (trans)esterification reactions, it acts as compatibilizer
 245 and plasticizer, thus improving the mixing and adhesion of the blend components. On the other hand,

246 the hydrolysis reactions produce volatiles responsible for the formation of porosities within the
247 films.(Carvalho et al., 2005)

248 To verify the occurrence of interactions among the blend components, ATR-FTIR analyses were
249 performed. The full infrared spectra ($3750\text{--}750\text{ cm}^{-1}$) of PBCEA, TPS and PBCEA/TPS blends are
250 collected in **Figure 3A**. In the blends, the absorption bands corresponding to the functional groups of
251 both main components are clearly visible, indicating that their chemical stability was not influenced
252 by the extrusion and filming treatment. A broad peak, typical of OH stretching vibration of inter- and
253 intra-molecular bonding of hydroxyl groups, is present at about 3350 cm^{-1} (**Figure 3B**).



254
255 **Figure 3.** ATR-FTIR spectra of PBCEA, TPS and PBCEA/TPS blends: A) full spectrum, B)
256 enlargement of the $3700\text{--}2500\text{ cm}^{-1}$ region and C) enlargement of the $1500\text{--}800\text{ cm}^{-1}$ region.

257

258 Its intensity depends on the samples' chemical composition. Specifically, the magnitude of the OH
 259 band for the PBCEA/TPS blends is within those of PBCEA (very low), and TPS (more intense).
 260 Further, higher concentrations of CA are shown to enhance this value.

261 All samples display aliphatic asymmetrical and symmetrical stretching C-H vibration peaks in the
 262 2840 – 3000 cm^{-1} region, although some differences can be evidenced. Specifically, with respect to
 263 PBCEA, PBCEA/TPS blends display one additional small peak located at 2900 cm^{-1} , assigned to C-
 264 H stretches of glycerol, and a shift of the more intense peak from 2923 cm^{-1} to 2943 cm^{-1} , due to the
 265 heterocyclic rings of starch.(Hablott et al., 2013) In addition, in the CA-containing blends, a shoulder
 266 at 2923 cm^{-1} can be observed, suggesting a better interaction among the blend components. The peak
 267 centered at 1721 cm^{-1} , relative to the carbonyl C=O stretching vibration of the PBCEA ester groups,
 268 is not significantly affected by the blending process. The fingerprint region (800 – 1500 cm^{-1} , **Figure**
 269 **3C**) contains useful information on the crystalline and amorphous regions in starch-based samples,
 270 respectively assigned to the bands located at 1047 and 1022 cm^{-1} .(Capron et al., 2007; Genovese et
 271 al., 2018)

272 While PBCEA and PBCEA/TPS samples were characterized by a major adsorption band at about
 273 1047 cm^{-1} , the peak at 1022 cm^{-1} is more marked in CA-containing blends, demonstrating an
 274 inversely proportional behavior of the TPS degree of crystallinity with the CA content, as already
 275 reported.(Genovese et al., 2018) Lastly, also the signal at 1000 cm^{-1} , relative to starch/water
 276 interactions, is more intense,(Capron et al., 2007) indicating that CA presence enhances the samples'
 277 water content.

278 To better analyse the behaviour of different blend films, their thermal stability and characteristic
 279 thermal transitions have been evaluated and the results are reported in **Table 2** and **Figure 4**.

280 PBCEA, notwithstanding the significant content of aliphatic sequences, shows high thermal stability,
 281 due to the presence of cycloaliphatic sub-units. In fact, similarly to PBCE,(Gigli et al., 2016) its
 282 degradation occurs in a single step leading to 100% mass loss above 650°C, and the maximum
 283 degradation temperature (T_{max}) is registered over 420°C (**Table 2**).

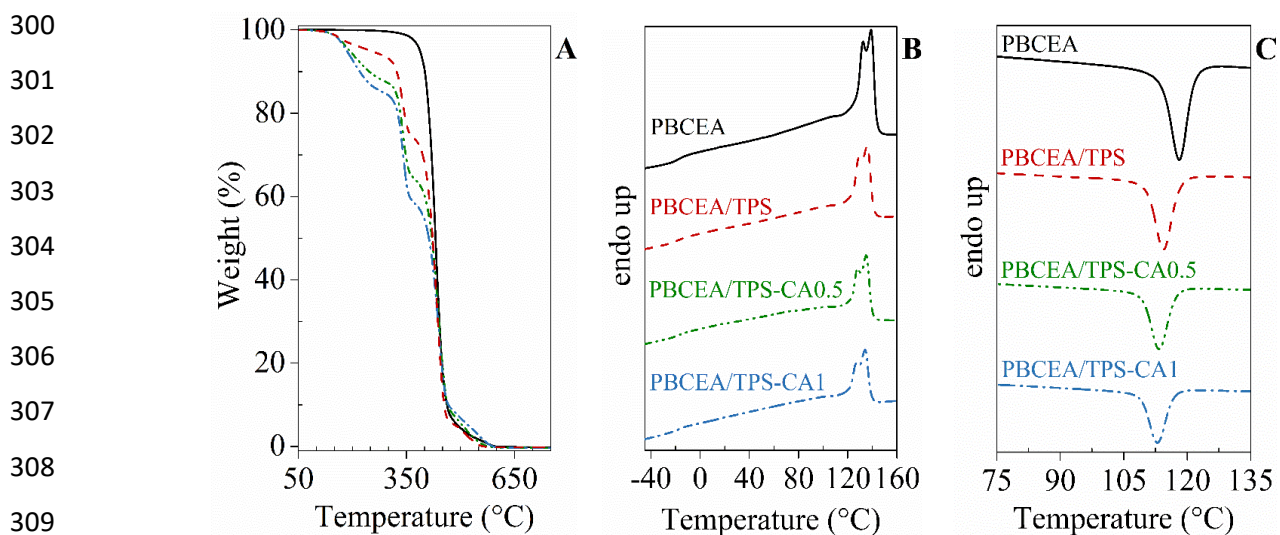
284

285 **Table 2.** Thermal properties of PBCEA and PBCEA/TPS blend films

	TGA				II scan, DSC				Cooling, DSC	
	$T_{\text{onset,I}}$ (°C)	$T_{\text{max,I}}$ (°C)	$T_{\text{onset,II}}$ (°C)	$T_{\text{max,II}}$ (°C)	T_{g} (°C)	ΔC_{p} ($\text{J}^{\circ}\text{C}^{-1}\text{g}^{-1}$)	T_{m} (°C)	ΔH_{m} (Jg^{-1})	T_{c} (°C)	ΔH_{c} (Jg^{-1})
PBCEA	/	/	405±1	431±2	-17±1	0.08±0.01	139±1	28±1	118±1	-28±1
PBCEA/TPS	326±1	341±1	406±1	437±1	-19±1	0.06±0.01	136±1	18±1	115±1	-19±1
PBCEA/TPS-CA0.5	325±1	340±1	407±2	439±1	-17±1	0.04±0.01	135±1	15±1	113±1	-15±1
PBCEA/TPS-CA1	323±2	341±1	405±1	439±1	-18±1	0.04±0.01	134±1	13±1	113±1	-13±1

286 On the other hand, the introduction of adipic acid subunits randomly distributed along the
287 poly(butylene cyclohexanedicarboxylate) (PBCE) chains caused significant reduction of the
288 copolymer glass transition and melting temperature, which respectively decreased of 29 and 28°C as
289 compared to PBCE.(Gigli, Lotti, et al., 2014; Gigli et al., 2016) In particular, the lowering of T_m
290 permitted the use of milder conditions for the blend processing, and thus the reduction of the kinetic
291 of unwanted starch degradation reactions.(W.-C. Liu et al., 2010)

292 The thermal stability profile of the blends, differently from PBCEA, is characterized by three weight
293 loss steps (**Figure 4A**), as previously observed.(Genovese et al., 2018) The first degradation segment,
294 below 150°C, is due to absorbed water evaporation. Then, before the second degradation step, a slight
295 decrease of weight, whose intensity well correlates with the CA content, can be observed in the
296 blends. This phenomenon might be due to the degradation of low molecular weight products
297 generated by the CA-mediated depolymerization action during extrusion. Lastly, the second ($T_{onset} =$
298 323 – 326°C) and the third step are respectively related to starch and PBCEA backbone degradation
299 (**Figure 4A**).



310 **Figure 4.** Thermogravimetric curves (A), II scan DSC (B) and crystallization exotherms (C) of
311 PBCEA and PBCEA/TPS blends

312

313 The CA addition also impacted the melting behavior of the PBCEA/TPS blends, while glass transition
314 remained unaffected (**Table 2**). Specifically, with the increase of CA load, a progressive decrease of
315 the melting temperature can be observed, indicating an improved dispersion of the TPS into the
316 PBCEA matrix, which in turn hampers the polyester crystals' perfection. (**Figure 4B**). Nevertheless,
317 PBCEA in the blends reaches the same degree of crystallization as in the pristine polymer, as
318 comparable ΔH_m are observed (it must be considered that the blends contain only 50% of PBCEA).
319 These results are further confirmed by analyzing the blends crystallization behavior (**Figure 4C**),

320 where a lowering of the crystallization temperature is recorded for PBCEA/TPS-CA0.5 and
 321 PBCEA/TPS-CA1 samples.

322 The analysis of surface wettability and moisture content that different formulations can absorb in
 323 specific environmental conditions is of great importance for packaging applications. These data
 324 acquire even more relevance due to the hydrophilic nature of thermoplastic starch, its brittleness, and
 325 high sensitivity to moisture, which limit its uses as packaging material.(Ivanič et al., 2019) **Table 3**
 326 summarizes the moisture content (MC) values of the different blends after 1 and 5 storage weeks at
 327 53% RH and 25°C. The MC of neat PBCEA film remained unchanged between 1 and 5 weeks,
 328 indicating that equilibrium conditions were already reached in the first week of storage, as described
 329 for other thermoplastic polymers.(A. Cano et al., 2016; A. I. Cano et al., 2015; F. Luzi et al., 2018;
 330 F. Luzi et al., 2017)

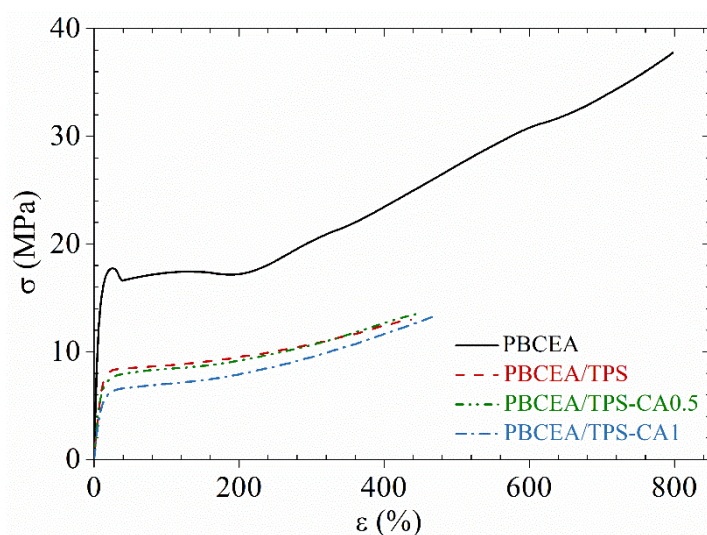
331 As expected, PBCEA blending with TPS induces an increase of MC, thus confirming what already
 332 indicated by ATR-FTIR. This phenomenon is related to the higher affinity of TPS to water with
 333 respect to PBCEA. Furthermore, the moisture content is enhanced by higher contents of CA, because
 334 of the plasticizing effect of this latter that influences the absorption of humidity,(Ivanič et al., 2019)
 335 being however, well below the reported values for CA-plasticized TPS, i.e. above 30%.(Jiugao et al.,
 336 2005) Also for the blends, after 5 weeks of storage, the MC data did not drastically vary as compared
 337 to those registered after 1 week (**Table 3**). However, while PBCEA/TPS displayed a lowering of the
 338 water content, in CA-containing samples the MC either slightly increased or remained constant,
 339 meaning that in these latter no significant retrogradation occurred over the monitored time span.
 340 Surface wettability data (**Table 3**) are in good agreement with MC and well correlate with the results
 341 of the ATR-FTIR analysis. In particular, TPS-containing samples are more hydrophilic than neat
 342 PBCEA, as due to a higher amount of hydroxyl groups.

343 **Table 3.** Water contact angle (WCA), moisture content and mechanical properties of PBCEA and
 344 PBCEA/TPS blends

	WCA (°)	Moisture content (% wt.)		Tensile properties				
		1 week	5 weeks	E (MPa)	σ_y (MPa)	ϵ_y (%)	σ_b (MPa)	ϵ_b (%)
PBCEA	81 ± 1	0.34±0.01	0.34±0.01	227 ± 18	18.6 ± 1.0	27 ± 1	37.7 ± 1.4	800 ± 50
PBCEA/TPS	76 ± 3	1.11±0.08	0.76±0.13	91 ± 8	/	/	12.2 ± 0.6	426 ± 27
PBCEA/TPS-CA0.5	76 ± 4	1.88±0.14	2.21±0.03	84 ± 1	/	/	12.8 ± 0.9	440 ± 40
PBCEA/TPS-CA1	70 ± 4	2.28±0.08	2.16±0.06	60 ± 7	/	/	12.7 ± 0.8	478 ± 16

345
 346 Even if TPS tensile characteristics can vary depending on the starch' source, its physicochemical
 347 properties, e.g. degree of crystallinity and T_g, and used plasticizer, it is not suited for high-

348 performance applications, as it displays very low tensile strength, of about 2-6 MPa, and elongation
 349 at break (ϵ_b) generally below 60-70%.(Cyras et al., 2008; Zhang et al., 2014) To verify if the blending
 350 with PBCEA resulted in improved mechanical behavior, tensile tests have been carried out on the
 351 prepared PBCEA/TPS blends. Representative stress-strain curves are reported in **Figure 5** and the
 352 results are contained in **Table 3**. PBCEA shows a typical hard and tough plastic behavior, with clearly
 353 visible yield and high elongation at break (**Table 3**). Therefore, with respect to PBCE homopolymer,
 354 for which ϵ_b equal to 30% and elastic modulus (E) of ca. 460 MPa have been described,(Gigli et al.,
 355 2013, 2016; Gigli, Govoni, et al., 2014) the introduction of flexible aliphatic co-units significantly
 356 modified its behavior, as E value halved and ϵ_b increased more than 26 times. Subsequent blending
 357 with TPS caused a further substantial variation of the tensile features of PBCEA, as the blends'
 358 behavior resemble **that** of elastomers. In fact, the yield point is not visible and a substantial drop of E
 359 (up to 4× lower for PBCEA/TPS-CA1), that gradually decreases with the increase of CA
 360 concentration due to the lower amount of crystalline domains (**Table 2**), can be observed. Elongation
 361 at break is lower than neat PBCEA, but higher than 400% in all cases, testifying the good
 362 compatibility among the blend components. A slight dependence on the CA concentration can be
 363 observed, too. Interestingly, the micro-porosity in the CA-containing samples does not compromise
 364 their tensile characteristics, as comparable stress at break and improved deformability with respect to
 365 the CA-free blend have been measured.

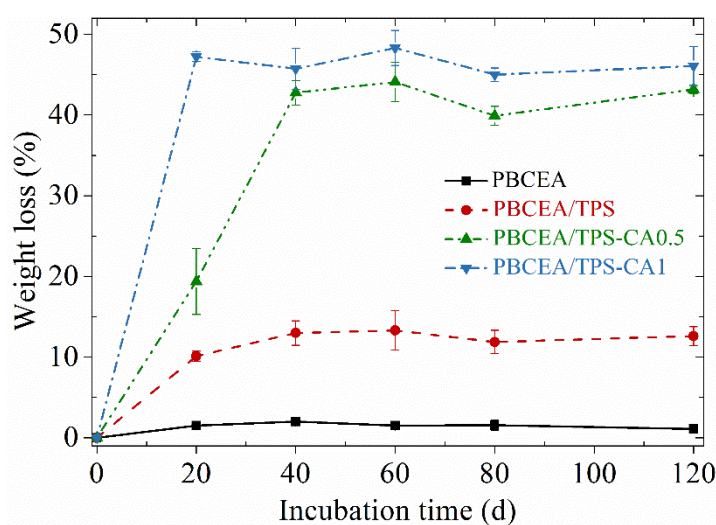


366
 367 **Figure 5.** Representative stress-strain curves of PBCEA and PBCEA/TPS blends
 368

369 These data acquire more value if compared to those of PBAT/TPS blend films recently
 370 reported.(Fourati et al., 2018) In this case, the addition of various concentrations of CA to 40/60
 371 blends caused a significant worsening of the performances, as the strength decreased from 10.2 to ca.
 372 3 MPa and ϵ_b declined from almost 200% to a maximum of 37%.

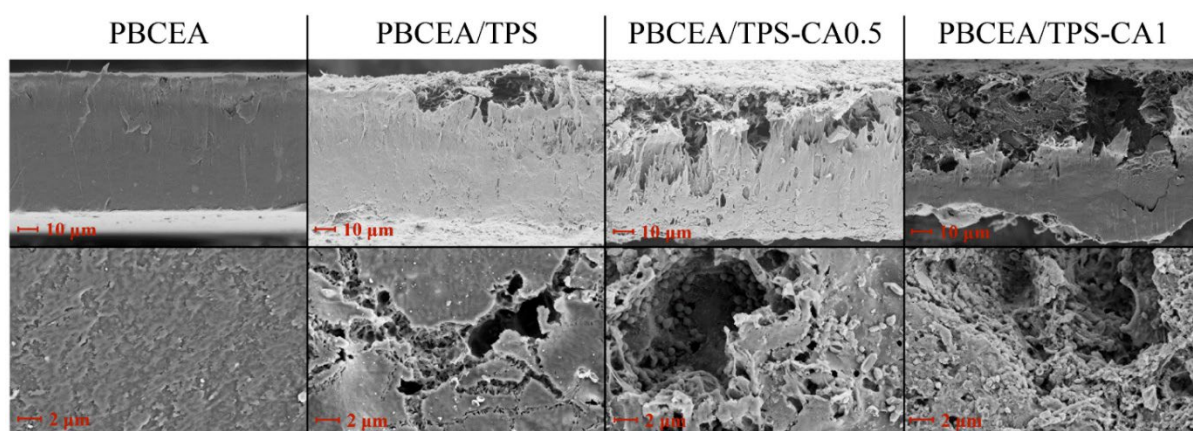
373 Last, but not least, the end of life fate of the PBCEA/TPS blends has been investigated through a lab-
374 scale composting test carried out over a 4 months' timeframe. Weight loss values (**Figure 6**) evidence
375 a clear dependence on the blend composition. Firstly, it can be observed that PBCEA does not
376 undergo any degradation in the time scale explored, and both film surface and cross section seem to
377 be unaffected by the incubation in compost (**Figure 7**). The result is not surprising because it was
378 previously demonstrated that substantial chemical modification of PBCE-based polyesters, e.g. by
379 the insertion of polar groups along the polymer backbone, is necessary to speed-up the biodegradation
380 process.(Genovese et al., 2016; Gigli, Lotti, et al., 2014)

381 Once again, the blending with 50% of TPS induced a significant change in the degradation kinetics
382 of the samples, which resulted further related to the CA content. In particular, the weight losses of
383 the blends are characterized by two well-distinct regions. In the first 30 – 40 days of incubation a
384 rapid increase of the weight loss has been observed, then followed by a flat trend. In the second part
385 of the experiment, no additional weight losses have been indeed recorded. Furthermore, while
386 PBCEA/TPS only reached about 15% loss, for both PBCEA/TPS-CA0.5 and PBCEA/TPS-CA1
387 values around 45%, almost equivalent to the whole TPS content, have been reached. However, some
388 differences can be highlighted, as the sample with a higher CA loading showed a much faster kinetic
389 of degradation. The results clearly indicate that TPS is much more easily degraded in CA containing
390 samples. This observation supports the above mentioned hypothesis that CA not only favors
391 transesterification reactions, thus improving blend compatibility, but also catalyzes TPS hydrolysis
392 during the extrusion process, which consequently facilitates the degradation process during
393 composting.(Carvalho et al., 2005) The higher the CA content, the greater the depolymerization
394 action on TPS, thus the faster the weight losses.



395
396 **Figure 6.** Gravimetric weight loss of PBCEA and PBCEA/TPS blends as a function of composting
397 time

398 SEM micrographs on partially degraded samples (**Figure 6**) confirmed the described trend. In fact,
399 both surface and cross section of PBCEA/TPS based blends appeared significantly affected by the
400 enzyme action.



401

402 **Figure 7.** FESEM micrographs of PBCEA and PBCEA/TPS blends after 120 d of incubation in
403 compost (top: cross section, bottom: film surface)

404

405 Cavities as big as a few microns, whose size and amount increases with the CA % wt., are fully visible
406 on the film surface. These holes deeply penetrate into the film thickness, reaching a depth of about
407 30 µm in PBCEA/TPS-CA1. The additional presence of micro-porosities may have exerted a positive
408 role in the process, by exposing a higher surface area to the enzymatic attack.

409

410 **4. Conclusions**

411 Films of PBCEA/TPS blends, containing a variable amount of citric acid, have been successfully
412 prepared. All components of the formulation contributed to the achievement of a novel ecofriendly
413 material with fully bio-based character, high flexibility, good moisture resistance and fast
414 degradability in compost.

415 Specifically, the introduction along the PBCE backbone of a specific amount of adipate co-units
416 revealed a winning strategy to modulate the melting temperature of the polyester matrix and enhance
417 the film flexibility, while maintaining sufficient crystallization ability and very good thermal stability.
418 In particular, the decrease of T_m allowed for the adoption of milder conditions during the melt
419 blending process, thus limiting the occurrence of unwanted starch degradation reactions.

420 In addition, the presence of CA had two positive effects: 1) compatibilization, through crosslinking
421 and (trans)esterification reactions, was confirmed by SEM analysis, which evidenced a better
422 interfacial adhesion between the two blend components, and by calorimetric studies that highlighted
423 a reduction of the crystallization ability of the PBCEA domains; 2) formation of micro-porosities,
424 due hydrolysis reactions, that, by increasing surface area, accelerated the water- and enzyme-

425 mediated fragmentation process under composting conditions, without having any detrimental effect
426 on the mechanical characteristics.

427

428 **CRedit authorship contribution statement**

429 F.Dominici: conceptualization, methodology; M.Gigli: conceptualization, methodology, data
430 curation, writing – original draft, review and editing; I.Armentano: investigation, validation, writing
431 – original draft; L.Genovese: investigation; F.Luzi: validation, resources; L.Torre: review; A.Munari:
432 resources, supervision; N.Lotti: conceptualization, supervision, writing - review and editing, project
433 administration.

434

435 **Conflict of interest**

436 The authors declare no conflict of interest.

437

438 **References**

- 439 Bulatović, V. O., Grgić, D. K., Slouf, M., Ostafinska, A., Dybal, J., & Jozinović, A. (2019).
440 Biodegradability of blends based on aliphatic polyester and thermoplastic starch. *Chemical*
441 *Papers*, 73(5), 1121–1134.
- 442 Cano, A., Cháfer, M., Chiralt, A., & González-Martínez, C. (2016). Development and
443 characterization of active films based on starch-PVA, containing silver nanoparticles. *Food*
444 *Packaging and Shelf Life*, 10, 16–24.
- 445 Cano, A. I., Cháfer, M., Chiralt, A., & González-Martínez, C. (2015). Physical and microstructural
446 properties of biodegradable films based on pea starch and PVA. *Journal of Food Engineering*,
447 167, 59–64.
- 448 Capron, I., Robert, P., Colonna, P., Brogly, M., & Planchot, V. (2007). Starch in rubbery and glassy
449 states by FTIR spectroscopy. *Carbohydrate Polymers*, 68(2), 249–259.
- 450 Carvalho, A. J. F., Zambon, M. D., da Silva Curvelo, A. A., & Gandini, A. (2005). Thermoplastic
451 starch modification during melt processing: Hydrolysis catalyzed by carboxylic acids.
452 *Carbohydrate Polymers*, 62(4), 387–390.

- 453 Cyras, V. P., Manfredi, L. B., Ton-That, M.-T., & Vázquez, A. (2008). Physical and mechanical
454 properties of thermoplastic starch/montmorillonite nanocomposite films. *Carbohydrate*
455 *Polymers*, 73(1), 55–63.
- 456 Fourati, Y., Tarrés, Q., Mutjé, P., & Boufi, S. (2018). PBAT/thermoplastic starch blends: Effect of
457 compatibilizers on the rheological, mechanical and morphological properties. *Carbohydrate*
458 *Polymers*, 199, 51–57.
- 459 Genovese, L., Dominici, F., Gigli, M., Armentano, I., Lotti, N., Fortunati, E., Siracusa, V., Torre, L.,
460 & Munari, A. (2018). Processing, thermo-mechanical characterization and gas permeability
461 of thermoplastic starch/poly(butylene trans-1,4-cyclohexanedicarboxylate) blends. *Polymer*
462 *Degradation and Stability*, 157, 100–107.
- 463 Genovese, L., Gigli, M., Lotti, N., Gazzano, M., Siracusa, V., Munari, A., & Dalla Rosa, M. (2014).
464 Biodegradable Long Chain Aliphatic Polyesters Containing Ether-Linkages: Synthesis, Solid-
465 State, and Barrier Properties. *Industrial & Engineering Chemistry Research*, 53(27), 10965–
466 10973.
- 467 Genovese, L., Soccio, M., Gigli, M., Lotti, N., Gazzano, M., Siracusa, V., & Munari, A. (2016). Gas
468 permeability, mechanical behaviour and compostability of fully-aliphatic bio-based
469 multiblock poly(ester urethane)s. *RSC Advances*, 6(60), 55331–55342.
- 470 Ghanbarzadeh, B., Almasi, H., & Entezami, A. A. (2011). Improving the barrier and mechanical
471 properties of corn starch-based edible films: Effect of citric acid and carboxymethyl cellulose.
472 *Industrial Crops and Products*, 33(1), 229–235.
- 473 Gigli, M., Govoni, M., Lotti, N., D. Giordano, E., Gazzano, M., & Munari, A. (2014). Biocompatible
474 multiblock aliphatic polyesters containing ether-linkages: influence of molecular architecture
475 on solid-state properties and hydrolysis rate. *RSC Advances*, 4(62), 32965–32976.
- 476 Gigli, M., Lotti, N., Gazzano, M., Siracusa, V., Finelli, L., Munari, A., & Dalla Rosa, M. (2013).
477 Fully Aliphatic Copolyesters Based on Poly(butylene 1,4-cyclohexanedicarboxylate) with

478 Promising Mechanical and Barrier Properties for Food Packaging Applications. *Industrial &*
479 *Engineering Chemistry Research*, 52(36), 12876–12886.

480 Gigli, M., Lotti, N., Gazzano, M., Siracusa, V., Finelli, L., Munari, A., & Rosa, M. D. (2014).
481 Biodegradable aliphatic copolyesters containing PEG-like sequences for sustainable food
482 packaging applications. *Polymer Degradation and Stability*, 105, 96–106.

483 Gigli, M., Lotti, N., Siracusa, V., Gazzano, M., Munari, A., & Dalla Rosa, M. (2016). Effect of
484 molecular architecture and chemical structure on solid-state and barrier properties of
485 heteroatom-containing aliphatic polyesters. *European Polymer Journal*, 78, 314–325.

486 Hablot, E., Dewasthale, S., Zhao, Y., Zhiguan, Y., Shi, X., Graiver, D., & Narayan, R. (2013).
487 Reactive extrusion of glycerylated starch and starch–polyester graft copolymers. *European*
488 *Polymer Journal*, 49(4), 873–881.

489 Ivanič, F., Kováčová, M., & Chodák, I. (2019). The effect of plasticizer selection on properties of
490 blends poly(butylene adipate-co-terephthalate) with thermoplastic starch. *European Polymer*
491 *Journal*, 116, 99–105.

492 Jiugao, Y., Ning, W., & Xiaofei, M. (2005). The Effects of Citric Acid on the Properties of
493 Thermoplastic Starch Plasticized by Glycerol. *Starch - Stärke*, 57(10), 494–504.

494 Kabir, E., Kaur, R., Lee, J., Kim, K.-H., & Kwon, E. E. (2020). Prospects of biopolymer technology
495 as an alternative option for non-degradable plastics and sustainable management of plastic
496 wastes. *Journal of Cleaner Production*, 258, 120536.

497 Kaseem, M., Hamad, K., & Deri, F. (2012). Thermoplastic starch blends: A review of recent works.
498 *Polymer Science Series A*, 54(2), 165–176. <https://doi.org/10.1134/S0965545X1202006X>

499 Khan, B., Niazi, M. B. K., Samin, G., & Jahan, Z. (2017). Thermoplastic Starch: A Possible
500 Biodegradable Food Packaging Material—A Review. *Journal of Food Process Engineering*,
501 40(3), e12447.

502 Lai, S.-M., Huang, C.-K., & Shen, H.-F. (2005). Preparation and properties of biodegradable
503 poly(butylene succinate)/starch blends. *Journal of Applied Polymer Science*, 97(1), 257–264.

- 504 Liu, F., Qiu, J., Wang, J., Zhang, J., Na, H., & Zhu, J. (2016). Role of cis -1,4-
505 cyclohexanedicarboxylic acid in the regulation of the structure and properties of a
506 poly(butylene adipate- co -butylene 1,4-cyclohexanedicarboxylate) copolymer. *RSC*
507 *Advances*, 6(70), 65889–65897.
- 508 Liu, H., Xie, F., Yu, L., Chen, L., & Li, L. (2009). Thermal processing of starch-based polymers.
509 *Progress in Polymer Science*, 34(12), 1348–1368.
- 510 Liu, W.-C., Halley, P. J., & Gilbert, R. G. (2010). Mechanism of Degradation of Starch, a Highly
511 Branched Polymer, during Extrusion. *Macromolecules*, 43(6), 2855–2864.
- 512 Luzi, F., Puglia, D., Dominici, F., Fortunati, E., Giovanale, G., Balestra, G. M., & Torre, L. (2018).
513 Effect of gallic acid and umbelliferone on thermal, mechanical, antioxidant and antimicrobial
514 properties of poly (vinyl alcohol-co-ethylene) films. *Polymer Degradation and Stability*, 152,
515 162–176.
- 516 Luzi, Francesca, Fortunati, E., Giovanale, G., Mazzaglia, A., Torre, L., & Balestra, G. M. (2017).
517 Cellulose nanocrystals from Actinidia deliciosa pruning residues combined with carvacrol in
518 PVA_CH films with antioxidant/antimicrobial properties for packaging applications.
519 *International Journal of Biological Macromolecules*, 104, 43–55.
- 520 Ojogbo, E., Ogunsona, E. O., & Mekonnen, T. H. (2020). Chemical and physical modifications of
521 starch for renewable polymeric materials. *Materials Today Sustainability*, 7–8, 100028.
- 522 Olivato, J. B., Müller, C. M. O., Carvalho, G. M., Yamashita, F., & Grossmann, M. V. E. (2014).
523 Physical and structural characterisation of starch/polyester blends with tartaric acid. *Materials*
524 *Science and Engineering: C*, 39, 35–39.
- 525 Ortega-Toro, R., Santagata, G., Gomez d’Ayala, G., Cerruti, P., Talens Oliag, P., Chiralt Boix, M.
526 A., & Malinconico, M. (2016). Enhancement of interfacial adhesion between starch and
527 grafted poly(ϵ -caprolactone). *Carbohydrate Polymers*, 147, 16–27.

528 Parulekar, Y., & Mohanty, A. K. (2007). Extruded Biodegradable Cast Films from
529 Polyhydroxyalkanoate and Thermoplastic Starch Blends: Fabrication and Characterization.
530 *Macromolecular Materials and Engineering*, 292(12), 1218–1228.

531 RameshKumar, S., Shaiju, P., O'Connor, K. E., & P, R. B. (2020). Bio-based and biodegradable
532 polymers - State-of-the-art, challenges and emerging trends. *Current Opinion in Green and*
533 *Sustainable Chemistry*, 21, 75–81.

534 Shi, R., Zhang, Z., Liu, Q., Han, Y., Zhang, L., Chen, D., & Tian, W. (2007). Characterization of
535 citric acid/glycerol co-plasticized thermoplastic starch prepared by melt blending.
536 *Carbohydrate Polymers*, 69(4), 748–755.

537 Skoog, E., Shin, J. H., Saez-Jimenez, V., Mapelli, V., & Olsson, L. (2018). Biobased adipic acid –
538 The challenge of developing the production host. *Biotechnology Advances*, 36(8), 2248–2263.

539 Wang, H., Wei, D., Zheng, A., & Xiao, H. (2015). Soil burial biodegradation of antimicrobial
540 biodegradable PBAT films. *Polymer Degradation and Stability*, 116, 14–22.

541 Wei, D., Wang, H., Xiao, H., Zheng, A., & Yang, Y. (2015). Morphology and mechanical properties
542 of poly(butylene adipate-co-terephthalate)/potato starch blends in the presence of synthesized
543 reactive compatibilizer or modified poly(butylene adipate-co-terephthalate). *Carbohydrate*
544 *Polymers*, 123, 275–282.

545 Yin, G.-Z., & Yang, X.-M. (2020). Biodegradable polymers: a cure for the planet, but a long way to
546 go. *Journal of Polymer Research*, 27(2), 38.

547 Zaaba, N. F., & Ismail, H. (2019). A review on tensile and morphological properties of poly (lactic
548 acid) (PLA)/ thermoplastic starch (TPS) blends. *Polymer-Plastics Technology and Materials*,
549 58(18), 1945–1964.

550 Zhang, Y., Rempel, C., & Liu, Q. (2014). Thermoplastic Starch Processing and Characteristics—A
551 Review. *Critical Reviews in Food Science and Nutrition*, 54(10), 1353–1370.

552